arXiv:1611.07031v1 [hep-ph] 21 Nov 2016

Neutral Weak Form Factors of Proton and Neutron

Raza Sabbir Sufian
Department of Physics and Astronomy, University of Kentucky, Lexington, KY 40506, USA

We determine the nucleon neutral weak electromagnetic form factors $G_{E,M}^{Z,p(n)}$ by combining results from light-front holographic QCD and lattice QCD calculations. We deduce the nucleon electromagnetic form factors from light-front holographic QCD and isolate the strange quark electromagnetic form factors $G_{E,M}^{s}$ using lattice QCD to obtain precise estimates of the neutral weak form factors in the momentum transfer range of $0\,\text{GeV}^2 \leq Q^2 \leq 0.5\,\text{GeV}^2$. From the lattice QCD calculation, we present Q^2-dependence of the strange quark form factors. This work presents, for the first time, predictions of the neutral weak Sachs electric form factors $G_{E}^{Z,p(n)}$ for both the proton and the neutron. We also deduce the neutral weak Dirac and Pauli form factors $F_{1,2}^{Z,p(n)}$ of the nucleon.

I. INTRODUCTION

In the electron elastic scattering from a hadron, parity-violating asymmetry arises from the interference of weak and electromagnetic amplitudes where the neutral weak current scattering is mediated by the Z-boson exchange. Because the weak current contains both vector and axial vector contributions, it violates parity and this property of the neutral weak current has been the main interest of the parity-violating (PV) experiments [1–13]. These PV experiments are important as they allow measurements of the Standard Model parameters related to Z-boson couplings and search for new PV interactions beyond the Standard Model. When electroweak (EW) radiative corrections [14, 15] are taken into account, the neutral weak electric and magnetic form factors $G_{E,M}^{Z,p}$ of the nucleon, under the assumption of isospin symmetry, can be expressed in terms of nucleon electric ($G_E^{\gamma,p(n)}$) and magnetic ($G_M^{\gamma,p(n)}$) form factors and a contribution from the strange (s) quarks as [3, 16–18],

$$G_{E,M}^{Z,p(n)}(Q^2) = \frac{1}{4}\Big[(1-4\sin^2\theta_W)(1+R_V^{p(n)})G_{E,M}^{\gamma,p(n)}(Q^2) - (1+R_V^{n(p)})G_{E,M}^{\gamma,n(p)}(Q^2) - (1+R_V^{(0)})G_{E,M}^{s}(Q^2)\Big], \quad (1)$$

where the subscript $E(M)$ stands for the electric(magnetic) form factor (FF) and the superscript $p(n)$ stands for the proton(neutron). Under the isospin symmetry, the strange electromagnetic form factor (EMFF) is the same for the proton and neutron, i.e. $G_{E,M}^{s,p} = G_{E,M}^{s,n} = G_{E,M}^{s}$. $R_V^{p(n)}$ and $R_V^{(0)}$ are radiative corrections to the vector form factors calculated in [14] and translated into the $\overline{\text{MS}}$-scheme in [15]. The updated analysis of these radiative corrections can be found in [19] and we use the values listed in [20] for the subsequent calculations.

The first measurement of the proton neutral weak magnetic form factor $G_M^{Z,p}$ from PV asymmetry in the polarized $\vec{e}-p$ scattering experiment was performed by the SAMPLE collaboration. Performed at a momentum transfer of $Q^2 = 0.1\,\text{GeV}^2$, the neutral weak magnetic form factor was found to be $G_M^{Z,p}(0.1\,\text{GeV}^2) = 0.34(11)$ nucleon magneton (n.m.) which corresponds to a value of $G_M^{s}(Q^2 = 0.1\,\text{GeV}^2) = 0.23(44)$ n.m [1]. These results were updated to obtain a value of $G_M^{s}(Q^2 = 0.1\,\text{GeV}^2) = 0.37(33)$ n.m. in [2]. An analysis of the SAMPLE data estimated $G_M^{Z,p}(0.1\,\text{GeV}^2) = 0.29(16)$ n.m. which corresponds to $G_M^{s}(Q^2 = 0.1\,\text{GeV}^2) = 0.49(65)$ n.m. [21]. A large positive value of G_M^{s} corresponds to a $G_M^{Z,p} < 0.40$ n.m. at $Q^2 = 0.1\,\text{GeV}^2$. However, the world data constrains that s-quarks contribute less than 6% and 5% to the magnetic moment and the mean-square charge radius of the proton respectively [22], and lattice QCD calculations favor a negative and small value of G_M^{s}. To date, no individual experiment provides high precision measurements of the nucleon neutral weak FFs in a wide range of Q^2. By considering the weak axial vector form factor G_A^e as an input, it is possible to separate the Sachs electric and magnetic FFs by combining PV asymmetry measurements from the experimental data. However, because of the complexity of the experiments, rather sizable uncertainties in the value G_A^e and the lack of knowledge of its Q^2 behavior, the extracted value of nucleon strange EMFFs from PV-asymmetry data vary widely in different experiments and global fits [20, 23, 24]. Although the typical EW radiative corrections are expected to be $\mathcal{O}(\alpha)$, the tree-level suppression of the interaction in the PV $\vec{e}-p$ scattering makes the radiative corrections to G_A^e more significant. The uncertainties in the radiative correction of G_A^e are large and the radiative corrections involving the strong interaction are not clearly known, extraction of $G_{E,M}^{Z,p(n)}$ from the PV scattering experiments is a tremendous challenge. One anticipates that with a reliable first-principles estimate of $G_{E,M}^{s}$, one can also give a prediction to the neutral weak FFs of the proton and the neutron according to Eq. (1).

The main goal of this article is to calculate the neutral weak FFs of the proton and the neutron $G_{E,M}^{Z,p(n)}$, $F_{1,2}^{Z,p(n)}$ by combining results of the strange quark EMFFs from the lattice QCD calculation in [25] and nucleon EMFFs calculated from the light-front holographic QCD in [26]. From the lattice QCD calculation, we isolate the s-quark contribution to the nucleon EMFFs and obtain the Q^2-dependence of the s-quark Sachs electric and magnetic FFs in the momentum transfer range of $0 \leq Q^2 \leq 0.5\,\mathrm{GeV}^2$. It has been shown in [26] that light-front holographic QCD can describe an extensive set of experimental data of the nucleon EMFFs in any momentum transfer range with high precision. Therefore, light-front holographic QCD becomes an eminent tool to calculate nucleon EMFFs in Eq. (1).

Light-front holographic QCD (LFHQCD) developed in Refs. [27–29] provides new insights into the quantitative determination of hadron mass spectra and FFs within a relativistic frame-independent first approximation to the light-front QCD Hamiltonian. This new approach to hadronic physics follows from the precise mapping of the Hamiltonian equations in the Anti-de Sitter (AdS) space to the relativistic semiclassical bound-state equations in the light front [28, 29]. This connection gives an exact relation between the holographic variable z of the AdS space and the invariant impact light-front variable ζ in the physical space-time [27, 28]. The LFHQCD approach incorporates superconformal quantum mechanics and captures the relevant aspects of color confinement based on a universal emerging single mass scale $\kappa = \sqrt{\lambda}$ [30–36]. In contrast to the AdS/CFT correspondence [37] where the baryon is an $SU(N_c)$ singlet bound state of N_c quarks in the large -N_c limit, in the LFHQCD approach baryons correspond to $N_c = 3$, and not the $N_c \to \infty$ limit [38]. Nucleon FFs determined within this nonperturbative framework incorporate vector dominance [39] at small Q^2 and correct leading twist-τ scaling or power law fall-off for hard scattering independent of the specific dynamics at large Q^2 [40, 41]. The most recent analysis of the nucleon EMFFs and their flavor-decomposition in the space-like region from LFHQCD shows remarkable agreement with the experimental data when effects of the pion cloud and SU(6) spin-flavor symmetry breaking for the neutron are considered [26]. With the confinement scale fixed by hadron spectroscopy and the anomalous magnetic moments of proton and neutron fixed by experiment, only 3 free parameters are necessary to describe an extensive set of data of the nucleon EMFFs. We refer to the work in Ref. [26] for the detailed analysis of the nucleon EMFFs from LFHQCD and these results will be used in the following calculations of this work.

Conventionally, we omit the unit nucleon magneton (n.m.) for the form factors in the rest of the paper.

II. NUCLEON ELECTROMAGNETIC FORM FACTORS IN LIGHT-FRONT HOLOGRAPHIC QCD

We now calculate nucleon EMFFs in the framework of light-front holographic QCD. The details of the calculation can be found in our recent work [26]. Considering pion cloud effect and breaking of SU(6) spin-flavor symmetry for the neutron Dirac FF, we write proton and neutron Dirac and Pauli FFs in terms of a different combination of twist operators following Ref. [26] as,

$$F_1^p(Q^2) = F_{\tau=3}(Q^2) \tag{2}$$
$$F_2^p(Q^2) = \chi_p[(1-\gamma_p)F_{\tau=4}(Q^2) + \gamma_p F_{\tau=6}(Q^2)], \tag{3}$$

for the proton, with $\chi_p = 1.793$ the proton anomalous moment, and

$$F_1^n(Q^2) = -\frac{1}{3} r \left[F_{\tau=3}(Q^2) - F_{\tau=4}(Q^2)\right], \tag{4}$$
$$F_2^n(Q^2) = \chi_n \left[(1-\gamma_n)F_{\tau=4}(Q^2) + \gamma_n F_{\tau=6}(Q^2)\right], \tag{5}$$

for the neutron, with $\chi_n = -1.913$ and $r = 2.08$ a free-parameter required to properly match to the experimental data as discussed in [26]. The twist-τ of a particle is defined here as the power behavior of its light-front wave function near $\zeta = 0$: $\Phi \sim \zeta^\tau$. For ground state hadrons the leading twist is the number of constituents. When computing nucleon FFs one has to constrain the asymptotic behavior of the leading fall-off of the FFs to match the twist of the nucleon's interpolating operator, *i.e.* $\tau = 3$, to represent the fact that at high virtualities the nucleon is essentially a system of 3 weakly interacting quarks. For a given twist τ, the FFs on the right-hand side in Eqs. (2)-(5) can be written by shifting the vector meson poles to their physical locations as

$$F_\tau(Q^2) = \frac{1}{\left(1+\frac{Q^2}{M^2_{\rho_{n=0}}}\right)\left(1+\frac{Q^2}{M^2_{\rho_{n=1}}}\right)\cdots\left(1+\frac{Q^2}{M^2_{\rho_{n=\tau-2}}}\right)}, \tag{6}$$

where

$$M^2_{\rho_n} = 4\kappa^2 \left(n + \frac{1}{2}\right), \; n = 0, 1, 2, ... \quad . \tag{7}$$

The ground-state mass of the ρ meson, $M_{\rho_{n=0}} \equiv M_\rho = 0.775\,\text{GeV}$ gives the value of $\kappa = M_\rho/\sqrt{2} = 0.548\,\text{GeV}$, where $\kappa = \sqrt{\lambda}$ is the emerging confinement scale [36]. Eq. (6) is expressed as a product of $\tau - 1$ poles along the vector meson Regge radial trajectory in terms of the ρ vector meson mass M_ρ and its radial excitations. The expression for the FF (6) contains a cluster decomposition: the hadronic FF factorizes into the $i = N - 1$ product of twist-2 monopole FFs evaluated at different scales [42] (N is the total number of constituents of a given Fock state):

$$F_i(Q^2) = F_{i=2}\left(Q^2\right)\; F_{i=2}\left(\tfrac{1}{3}Q^2\right) \cdots F_{i=2}\left(\tfrac{1}{2i-1}Q^2\right). \tag{8}$$

Keeping in mind that the gauge-gravity duality does not determine the spin-flavor structure of the nucleons, this one is conventionally included in the nucleon wave function using SU(6) spin-flavor symmetry. The departure of the free-parameter r from unity may be interpreted as a SU(6) symmetry breaking effects in the neutron Dirac FF. Eqs. (2) and (4) are the SU(6) results for the spin non-flip nucleon FFs in the valence configuration [38, 43]. Eqs. (3) and (5) correspond to the extension of the phenomenological spin-flip nucleon FFs described in Refs. [38, 43] and which incorporate the effect of twist-6 Fock components, i.e. the contribution of $|qqqq\bar{q}\rangle$ components in the nucleon Pauli FFs. We obtain the probabilities $\gamma_p = 0.27$ in Eq. (3) and $\gamma_n = 0.38$ in Eq. (5) by fitting the experimental data. The additional parameter r accounts for the SU(6) symmetry breaking effects in the neutron and $r = 2.08$ gives a proper match to the experimental data. We show in Fig. 6 and in Ref. [26] that nucleon EMFFs can be calculated very accurately using the above FF expressions and the available experimental data for both the proton and neutron at low and high Q^2 are described very well. Comparison of LFHQCD prediction of the nucleon FFs with other experimental data and flavor decomposition of the nucleon FFs can be found in Ref. [26]. Therefore, we use the LFHQCD formalism to calculate nucleon EMFFs in obtaining the nucleon neutral weak FFs.

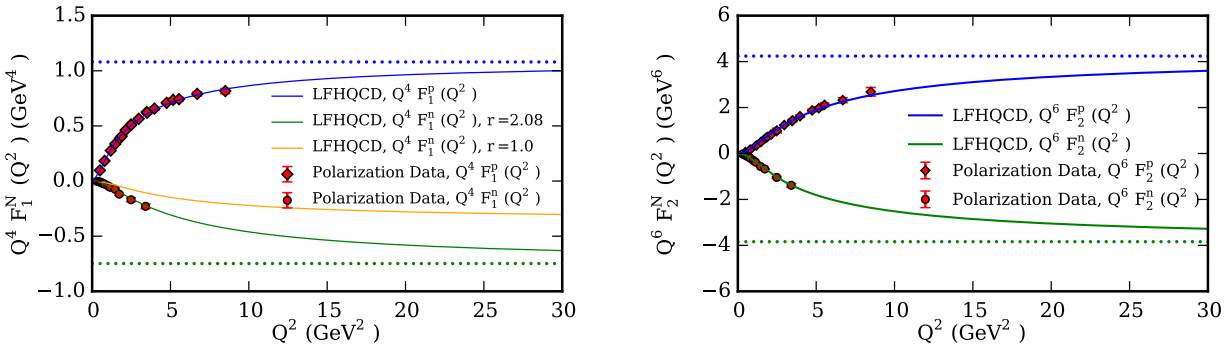

(a) Nucleon Dirac FFs from LFHQCD multiplied by Q^4

(b) Nucleon Pauli FFs from LFHQCD multiplied by Q^6

FIG. 1. Comparison of the LFHQCD results with selected world data for the Dirac and Pauli form factors for the proton and neutron. The orange line corresponds to the SU(6) symmetry limit for the neutron Dirac form factor. The dotted lines are the asymptotic predictions from LFHQCD. References to the experimental data are given in [26].

The nucleon Sachs EMFFs are written as linear combinations of the Dirac and Pauli FFs as following:

$$G_E^{\gamma,p(n)}(Q^2) = F_1^{\gamma,p(n)}(Q^2) - \frac{Q^2}{4m_N^2} F_2^{\gamma,p(n)}(Q^2),$$
$$G_M^{\gamma,p(n)}(Q^2) = F_1^{\gamma,p(n)}(Q^2) + F_2^{\gamma,p(n)}(Q^2), \tag{9}$$

which will be used to obtain nucleon neutral weak Sachs EMFFs in Eq. (1).

A. Model Uncertainties

LFHQCD, constrained by superconformal quantum mechanics [34], yields a semiclassical description of QCD that can be regarded as a first approximation to the full QCD. Therefore, for example, logarithmic terms due to quantum

loops are absent in the model. This is reflected by the fact that the fitted values of the universal confinement scale $\kappa = \sqrt{\lambda}$ differ by about 10% for different trajectories [31]. We obtain from the ρ -trajectory the value $\kappa = 0.537$ GeV, for the nucleon trajectory $\kappa = 0.499$ GeV, and from a fit to the ρ -mass alone $\kappa = m_\rho/\sqrt{2} = 0.548$ GeV. Since the ρ -pole is dominant for the nucleon FFs, we take this latter value as the default value in our calculation. However, for the low Q^2 region, the form of the nucleon wave function is important. Therefore we estimate the uncertainty in this region from the difference of the results obtained with the default value of $\kappa = 0.548$ GeV and the result obtained with $\kappa = 0.499$ GeV from the nucleon trajectory. We also consider the uncertainty of the nucleon FF by using the zero-probabilities ($\gamma_p = \gamma_n = 0$) of the higher Fock components in the Pauli FFs. In the low-energy domain of our calculation, i.e. for $Q^2 \leq 0.5\,\mathrm{GeV}^2$, the largest uncertainty comes from the difference in κ-values and the uncertainty due to higher Fock components are very small.

III. STRANGE QUARK FORM FACTORS FROM LATTICE QCD

We have calculated the strange quark contribution to nucleon's magnetic moment and charge radius in Ref. [25] using the overlap fermion on the $(2+1)$ flavor RBC/UKQCD domain wall fermion (DWF) gauge configurations. Details of these ensembles are listed in Table I. We use 24 valence quark masses in total for the 24I, 32I, 32ID, and 48I ensembles representing pion masses in the range $m_\pi \in$(135, 400) MeV to explore the quark-mass dependence of the s-quark FFs.

Ensemble	$L^3 \times T$	a (fm)	$m_s^{(s)}$(MeV)	m_π (MeV)	N_{config}
24I [44]	$24^3 \times 64$	0.1105(3)	120	330	203
32I [44]	$32^3 \times 64$	0.0828(3)	110	300	309
32ID [45]	$32^3 \times 64$	0.1431(7)	89.4	171	200
48I [45]	$48^3 \times 96$	0.1141(2)	94.9	139	81

TABLE I. The parameters for the DWF configurations: spatial/temporal size, lattice spacing [44, 45], the sea strange quark mass under $\overline{\mathrm{MS}}$ scheme at 2 GeV, the pion mass corresponding to the degenerate light sea quark mass and the numbers of configurations used in this work.

One can perform the model-independent $z-$expansion fit [46, 47]

$$G^{s,z-exp}(Q^2) = \sum_{k=0}^{k_{max}} a_k z^k,\ z = \frac{\sqrt{t_{\rm cut}+Q^2} - \sqrt{t_{\rm cut}}}{\sqrt{t_{\rm cut}+Q^2} + \sqrt{t_{\rm cut}}}, \tag{10}$$

using the lattice data to extrapolate the s-quark magnetic moment and charge radius as shown in [25] and then use the fit parameters a_k to interpolate $G^s_{E,M}$ values at various Q^2 for a given valence quark mass on the lattice. The available Q^2 on the 24I and 32I ensembles are $Q^2 \in (0.22, 1.31)\,\mathrm{GeV}^2$, on the 32ID ensemble are $Q^2 \in (0.07, 0.43)\,\mathrm{GeV}^2$ and on the 48I ensemble are $Q^2 \in (0.05, 0.31)\,\mathrm{GeV}^2$. It is a common problem for lattice QCD calculations that the signal-to-noise-ratio decreases as one reaches the physical pion mass. From our study, we also find that the lattice results of $G^s_{E,M}(Q^2)$ near the physical pion mass $m_\pi = 140\,\mathrm{MeV}$ for the 48I ensemble [45] is noisier compared to the lattice ensembles with heavier pion mass. Therefore, an extrapolation of the 48I ensemble lattice data to obtain $G^s_{E,M}$ at $Q^2 \gg 0.31\,\mathrm{GeV}^2$ can be unreliable and we restrict ourselves to, up to $Q^2 = 0.5\,\mathrm{GeV}^2$ while extrapolating the $G^s_{E,M}$ beyond $Q^2 = 0.31\,\mathrm{GeV}^2$. It is important to note that the lattice QCD estimate of $G^s_{E,M}(Q^2)$ we present here is the most precise and accurate first-principles calculation of s-quark EMFFs to date. This is the only calculation at the physical pion mass where we have considered the quark mass dependence, with finite lattice spacing, volume corrections, and partial quenching effect to determine the s-quark EMFFs.

After the Q^2-interpolation, for a given Q^2 -value, we obtain 24 data points corresponding to different valence quark masses from 3 different lattice spacings and volumes and 4 sea quark masses including one at the physical point. We use chiral extrapolation formula following Ref. [48] and volume correction following Ref. [49]. The empirical formula for the global fit of the strange quark Sachs electric FF at a given Q^2 is

$$G^s_E(m_\pi, m_K, m_{\pi,vs}, a, L) = A_0 + A_1 m_K^2 + A_2 m_\pi^2 + A_3 m_{\pi,vs}^2 + A_4 a^2 + A_5 \sqrt{L} e^{-m_\pi L}, \tag{11}$$

where m_π/m_K is the valence pion/kaon mass and $m_{\pi,vs}$ is the partially quenched pion mass $m^2_{\pi,vs} = 1/2(m^2_\pi + m^2_{\pi,ss})$ with $m_{\pi,ss}$ the pion mass corresponding to the sea quark mass. The $\chi^2/d.o.f.$ for different Q^2 global fit ranges between 0.7-1.13. For example, in the continuum limit, the global fit for $Q^2 = 0.25\,\mathrm{GeV}^2$ results in the physical value

of $G_E^s|_{phys} = 0.0024(8)$, $A_1 = 0.58(30)$, $A_2 = -0.29(15)$, $A_3 = -0.003(9)$, $A_4 = 0.001(2)$, and $A_5 = -0.001(3)$ with $\chi^2/d.o.f. = 1.1$. One can consider the $\log(m_K)$-term in the chiral extrapolation of G_E^s as shown in [48], however our analysis shows that this term does not have any effect on the global fit for our lattice data. A similar vanishing difference has been observed if one considers $e^{-m_\pi L}$ instead of $\sqrt{L}e^{-m_\pi L}$ term in the volume correction. For example, including the factor $\log(m_K)$ and $e^{-m_\pi L}$ instead of $\sqrt{L}e^{-m_\pi L}$ one obtains, $G_E^s|_{phys} = 0.0026$ in comparison with $G_E^s|_{phys} = 0.0024$ we get from (11). We include these small effects in the systematics of the global fit results. We also consider a 20% systematic uncertainty from the model-independent z-expansion interpolation coming from adding a higher order term a_3 while fitting the $G_E^s(Q^2)$ data. These uncertainties from the empirical fit formula and z-expansion are added to the systematics discussed in [25].

FIG. 2 shows the Q^2-dependence of the s-quark Sachs electric form factor G_E^s in the continuum limit, i.e. $m_\pi = m_{\pi,vs} \to 140\,\text{MeV}$, $a \to 0$, and $L \to \infty$ with the statistical and systematic uncertainties. The nonzero value of the strange Sachs electric form factor G_E^s at any $Q \neq 0$ means that the spatial distribution of the s and $\bar{s}$ quarks are not the same in the nucleon. If the distributions of the s and $\bar{s}$ quarks were the same, their contribution to the nucleon electric FF would have the same magnitude with opposite signs. Since the net strangeness in the nucleon is zero, we have $G_E^s = 0$ at $Q^2 = 0$.

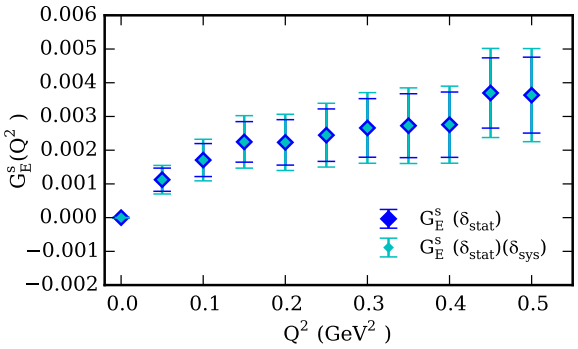

FIG. 2. Q^2-dependence of the strange Sachs electric form factor. The blue error bars indicate the statistical uncertainties and the cyan error bars indicate the statistical and systematic uncertainties added in quadrature.

Similarly, we calculate the strange Sachs magnetic form factor G_M^s at a particular Q^2 using the following global fit formula

$$G_M^s(m_\pi, m_K, m_{\pi,vs}, a, L) = A_0 + A_1 m_\pi + A_2 m_K + A_3 m_{\pi,vs}^2 + A_4 a^2 + A_5 m_\pi (1 - \frac{2}{m_\pi L}) e^{-m_\pi L}, \tag{12}$$

where we have used a chiral extrapolation linear in m_π and $m_{\text{loop}} = m_K$ [48, 50–52]. For the volume correction we refer to Ref. [53]. From the global fit formula (12), for example, in the continuum limit at $Q^2 = 0.25\,\text{GeV}^2$, we obtain $G_M^s|_{phys} = -0.018(4)$, $A_1 = 0.04(3)$, $A_2 = -0.18(12)$, $A_3 = -1.27(84)$, $A_4 = 0.008(6)$, and $A_5 = 0.04(5)$ with $\chi^2/d.o.f. = 1.13$. From the fitted values of the parameters in the global fit formula (12), it is seen that the quark mass dependencies play an important role in calculating $G_M^s(Q^2)$ at the physical point. A 9% systematic uncertainty from the model-independent $z-$expansion and an uncertainty from the empirical fit formula have been included as discussed in [25]. We obtain systematics from the global fit formula by replacing the volume correction by $e^{-m_\pi L}$ only and also by adding $m_{\pi,vs}$ term in the fit and include the difference in the systematics of the global fit results. The results of $G_M^s(Q^2)$ in the continuum limit are presented in FIG. 3.

IV. CALCULATION OF NEUTRAL WEAK FORM FACTORS

Since the neutral weak Z-boson can have both vector and axial vector interactions, the amplitude of the Z-exchange can have both parity-conserving and parity-violating components. The parity-conserving and parity-violating Z-amplitudes in the electron-nucleon scattering can be written as

$$\mathcal{M}_Z^{PC} = \frac{G_F}{2\sqrt{2}}(g_V^i l^\mu J_\mu^Z + g_A^i l^{\mu 5} J_{\mu 5}^Z), \tag{13}$$

$$\mathcal{M}_Z^{PV} = \frac{G_F}{2\sqrt{2}}(g_V^i l^\mu J_{\mu 5}^Z + g_A^i l^{\mu 5} J_\mu^Z), \tag{14}$$

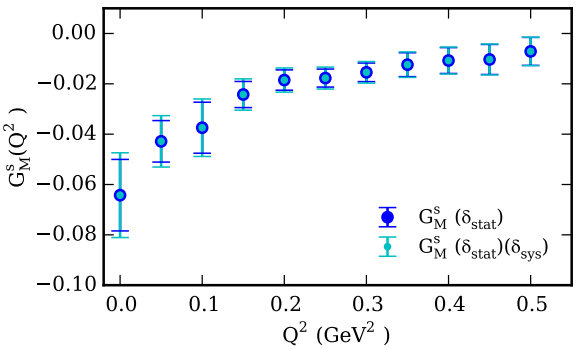

FIG. 3. Q^2-dependence of the strange Sachs magnetic form factor. The blue error bars indicate the statistical uncertainties and the cyan error bars indicate the statistical and systematic uncertainties added in quadrature.

where G_F is the Fermi constant, $g^i_{V(A)}$ the weak vector(axial) charge of the fermions, $l^\mu(l^{\mu 5})$ the leptonic vector(axial) current, and $J^Z_\mu(J^Z_{\mu 5})$ the nucleon vector(axial) current. In the electron-nucleon elastic scattering, the first-order interactions are mediated either by a photon(γ) or a neutral weak Z-boson as shown in FIGs. 4a and 4b. The contributions to the weak FFs from additional diagrams in FIGs. 4c and 4d should also be considered. Moreover, there can be contributions that involve strong interactions where γ and Z-boson can interact with several quarks and these diagrams are not shown here. These "many-quark" corrections are target specific and difficult to calculate; the calculations are model-dependent.

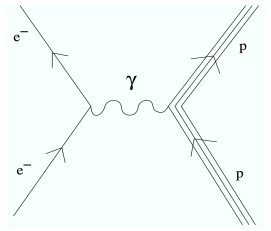

(a) Tree-level EM Feynman diagrams in elastic electron-nucleon scattering mediated by photon

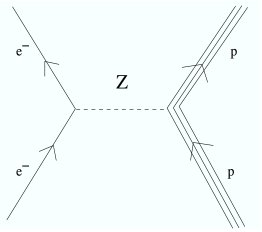

(b) Tree-level weak Feynman diagrams in elastic electron-nucleon scattering mediated by neutral weak Z-boson

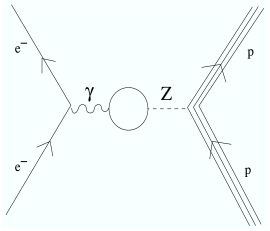

(c) Feynman diagram representing "one-quark" radiative correction: vacuum polarization with leptons in the loop

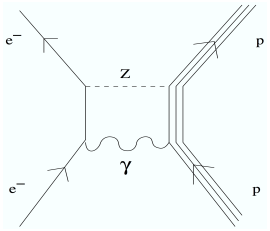

(d) Feynman diagram representing "one-quark" radiative correction: $\gamma - Z$ box diagram

FIG. 4. Feynman diagrams representing tree-level EM and weak interactions and "one-quark" radiative corrections.

We use the LFHQCD predictions of $G^{\gamma,p(n)}_{E,M}(Q^2)$ from Eq. (9) and $G^s_{E,M}(Q^2)$ from lattice QCD calculation in Eq. (1) to obtain the nucleon neutral weak FFs which are shown in FIGs. 5 and 6. While in the EM charge coupling, the electron couples to the proton and neutron with strengths 1 and 0 respectively, in the weak interaction the Z-coupling with the neutron is larger than the coupling to the proton. This can be seen from FIGs. 5 and 6: neutron weak FFs are larger than the proton weak FFs. As shown in FIG. 5, our prediction of the proton neutral weak FF at $Q^2 \approx 0.1\text{GeV}^2$ is within the uncertainty of the experimental measurement by the SAMPLE collaboration $G^{Z,p}_M(0.1\,\text{GeV}^2) = 0.34(11)$ [1] but with better precision and the central value differs significantly. It is important to note that, a positive value of $G^s_M(Q^2)$ leads to a $G^{Z,p}_M < 0.40$ and a negative $G^s_M(Q^2)$ leads to a $G^{Z,p}_M > 0.40$ at $Q^2 = 0.1\,\text{GeV}^2$. $G^{Z,p}_M(0.1\,\text{GeV}^2) = 0.34(11)$ measured in [1] corresponds to a value of $G^s_M(Q^2 = 0.1\,\text{GeV}^2) = 0.23(44)$ and an updated value of $G^s_M(Q^2 = 0.1\,\text{GeV}^2) = 0.37(33)$ can be found in [2]. An analysis of the SAMPLE data estimated $G^{Z,p}_M(0.1\,\text{GeV}^2) = 0.29(16)$ [21].

No experimental or theoretical estimates of the proton neutral weak electric FF and the neutron neutral weak electric and magnetic FFs have been reported in the literature to be compared with the calculated values in this work. It is interesting to note that the neutral weak electric Sachs FF of the neutron $G^{Z,n}_E$ is significantly larger in magnitude than that of the proton, seen FIG. 6. It can be seen in FIG. 6b that $G^{Z,p}_E$ becomes negative around

$Q^2 = 0.25\,\mathrm{GeV}^2$.

For the interaction shown in FIG. 4b to violate parity, one coupling of Z must be vector and the other must be axial vector. When interpreting the data from parity-violating experiment, one has to consider the weak axial charge G_A^e. However, its value is experimentally unknown and the radiative corrections to this term can be as large as $\sim 100\%$, because the strong interaction effects cannot be precisely calculated [54]. In principle, one can constrain both G_M^s and G_A^e in a measurement of the PV asymmetry in $\vec{e} - N$ scattering, but a free neutron target is not available at this moment. Therefore, an easier and efficient way to calculate the nucleon neutral weak FF is to isolate the strange quark EMFFs using a first-principles calculation where no prior knowledge of G_A^e is required. One can thus obtain the neutral weak FFs using Eq. (1) given that the nucleon total EMFFs are known as described in our approach. A model-dependent prediction of the proton neutral weak magnetic form factor can be found in Refs. [55, 56].

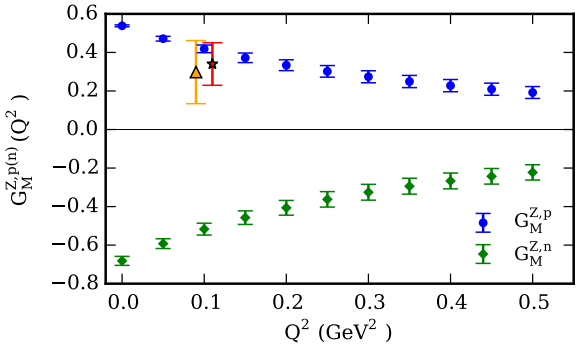

FIG. 5. Q^2-dependence of the proton and neutron neutral weak magnetic form factor $G_M^{Z,p(n)}$. The statistical and systematic uncertainties from the lattice QCD calculation of $G_{E,M}^s$ and the systematic uncertainties from the LFHQCD model have been added in quadrature. The red star is the experimental result from [1] and the orange triangle is from the analysis of SAMPLE proton data performed in [21] at $Q^2 = 0.1\,\mathrm{GeV}^2$ (with offset Q^2 for visibility).

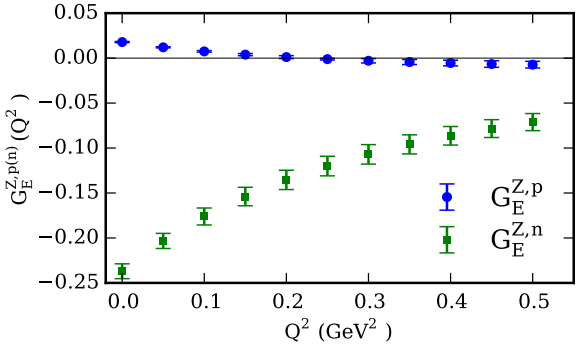

(a) Neutral weak Sachs electric form factor of the nucleon

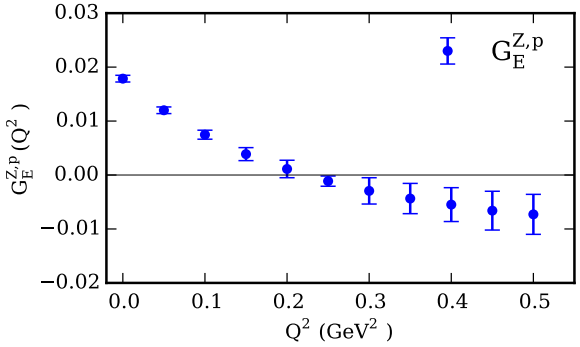

(b) Neutral weak Sachs electric form factor of the proton

FIG. 6. Q^2-dependence of the proton and neutron neutral weak electric form factor $G_E^{Z,p(n)}$. The $G_E^{Z,p}(Q^2)$ plot is shown separately in FIG. 6b for better visibility in comparison with the $G_E^{Z,n}(Q^2)$ data. The statistical and systematic uncertainties from the lattice QCD calculation of $G_{E,M}^s$ and the systematic uncertainties from the LFHQCD model have been added in quadrature.

We now deduce neutral weak Dirac and Pauli FFs from the above calculation of neutral weak Sachs EMFFs using Eq. (9). The results are shown in FIGs. 7 and 8. Similar to the signal-to-noise ratio of the $G_E^{Z,p}(Q^2)$, the signal-to-noise ratio for the proton neutral weak Dirac form factor $F_1^{Z,p}(Q^2)$ decreases with Q^2 and the precision is about 3σ at $Q^2 = 0.5\,\mathrm{GeV}^2$ after the systematic uncertainties are added in quadrature with the statistical uncertainties. These values of the neutral weak FFs are yet to be compared with future experimental determinations since currently these values are experimentally unknown.

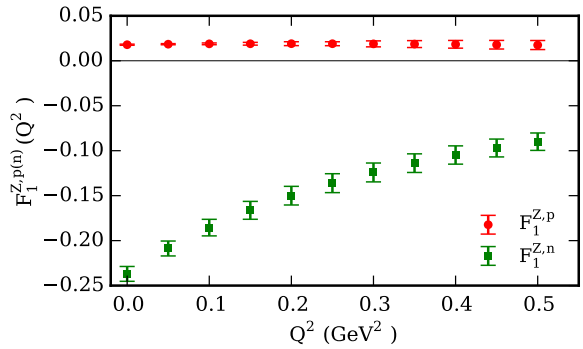

(a) Neutral weak Dirac FF of the nulceon

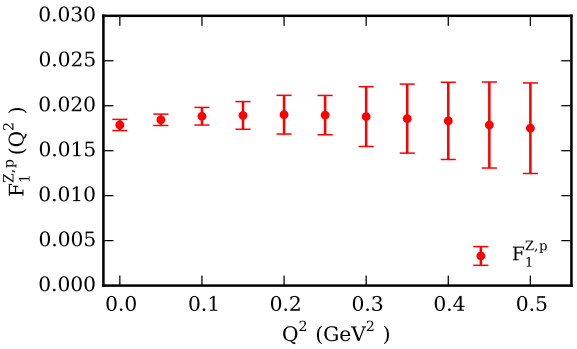

(b) Neutral weak Dirac FF of the proton

FIG. 7. Q^2-dependence of the proton and neutron neutral weak Dirac form factor $F_1^{Z,p(n)}$. The $F_1^{Z,p}(Q^2)$ plot is shown separately in FIG. 7b for better visibility in comparison with the $F_1^{Z,n}(Q^2)$ data. Statistical and systematic uncertainties are added in quadrature to obtain the final uncertainty.

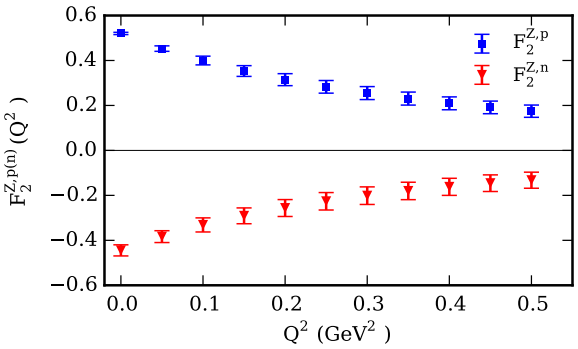

FIG. 8. Q^2-dependence of the proton and neutron neutral weak Dirac form factor $F_2^{Z,p(n)}$. Statistical and systematic uncertainties are added in quadrature to obtain the final uncertainty.

V. CONCLUSIONS

This analysis presents the first determination of the Q^2-dependence of the neutral weak electromagnetic form factors. The nucleon neutral weak form factors have been calculated in the momentum transfer range of $0\,\mathrm{GeV}^2 \leq Q^2 \leq 0.5\,\mathrm{GeV}^2$ by combining results from light-front holographic QCD and lattice QCD calculations. We have presented a first-principles determination of the Q^2-dependence of the strange quark form factors at the physical pion mass $m_\pi = 140$ MeV and in the continuum limit. With a model-independent extraction of the Q^2-dependence of the strange quark form factors, 24-valence quark masses including at the physical pion mass have been used to explore the quark mass dependence and with finite lattice spacing and volume corrections to determine the strange quark form factors from lattice QCD calculation. Since the strange quark contribution to nucleon electromagnetic form factors are constrained to be small by the global experimental data, and a similar small contribution has been confirmed by first-principles lattice QCD calculations, a precise experimental determination of the neutral weak form factors from parity violating experiments will be challenging. The lattice results of the strange quark form factors at the physical point and light-front holographic QCD prediction of the nucleon electromagnetic form factors have been used to determine the nucleon neutral weak form factors precisely. The determination of neutral weak form factors in this way does not require a prior knowledge of the weak axial form factor and its higher order radiative corrections which are less accurately constrained. Given our precise predictions for the neutral weak electromagnetic form factors at the physical point, we anticipate these results will be verified by future precision experiments.

ACKNOWLEDGMENTS R.S.S. thanks the RBC/UKQCD collaborations for providing their DWF gauge configurations. R.S.S. also thanks Stanley J Brodsky, John Connell, Sumit R. Das, Alexandre Deur, Terrence Draper,

Hasnain Hafiz, Keh-Fei Liu, Tianbo Liu, Sumiran Pujari, Omer Rahman, and Guy F. de Téramond who provided insight and expertise that greatly assisted the research. This work is supported in part by the U.S. DOE Grant No. DE-SC0013065. This research used resources of the Oak Ridge Leadership Computing Facility at the Oak Ridge National Laboratory, which is supported by the Office of Science of the U.S. Department of Energy under Contract No. DE-AC05-00OR22725.

---

[1] B. Mueller *et al.* [SAMPLE Collaboration], "Measurement of the proton's neutral weak magnetic form-factor," Phys. Rev. Lett. **78**, 3824 (1997) [arXiv:nucl-ex/9702004].
[2] D. T. Spayde *et al.* [SAMPLE Collaboration], "The Strange quark contribution to the proton's magnetic moment," Phys. Lett. B **583**, 79 (2004) [arXiv:nucl-ex/0312016].
[3] E. J. Beise, M. L. Pitt and D. T. Spayde, "The SAMPLE experiment and weak nucleon structure," Prog. Part. Nucl. Phys. **54**, 289 (2005) [arXiv:nucl-ex/0412054].
[4] K. A. Aniol *et al.* [HAPPEX Collaboration], "Parity violating electroweak asymmetry in polarized-e p scattering," Phys. Rev. C **69**, 065501 (2004) [arXiv:nucl-ex/0402004].
[5] F. E. Maas *et al.* [A4 Collaboration], "Measurement of strange quark contributions to the nucleon's form-factors at $Q^2 = 0.230(\mathrm{GeV/c})^2$," Phys. Rev. Lett. **93**, 022002 (2004) [arXiv:nucl-ex/0401019].
[6] F. E. Maas *et al.*, "Evidence for strange quark contributions to the nucleon's form-factors at $Q^2 = 0.108(\mathrm{GeV/c})^2$," Phys. Rev. Lett. **94**, 152001 (2005) [arXiv:nucl-ex/0412030].
[7] K. A. Aniol *et al.* [HAPPEX Collaboration], "Parity-violating electron scattering from He-4 and the strange electric form-factor of the nucleon," Phys. Rev. Lett. **96**, 022003 (2006) [arXiv:nucl-ex/0506010].
[8] K. A. Aniol *et al.* [HAPPEX Collaboration], "Constraints on the nucleon strange form-factors at $Q^2 \sim 0.1\,\mathrm{GeV}^2$," Phys. Lett. B **635**, 275 (2006) [arXiv:nucl-ex/0506011].
[9] D. S. Armstrong *et al.* [G0 Collaboration], "Strange quark contributions to parity-violating asymmetries in the forward G0 electron-proton scattering experiment," Phys. Rev. Lett. **95**, 092001 (2005) [arXiv:nucl-ex/0506021].
[10] A. Acha *et al.* [HAPPEX Collaboration], "Precision Measurements of the Nucleon Strange Form Factors at $Q^2 \sim 0.1\,\mathrm{GeV}^2$," Phys. Rev. Lett. **98**, 032301 (2007) [arXiv:nucl-ex/0609002].
[11] D. Androic *et al.* [G0 Collaboration], "Strange Quark Contributions to Parity-Violating Asymmetries in the Backward Angle G0 Electron Scattering Experiment," Phys. Rev. Lett. **104**, 012001 (2010) [arXiv:0909.5107 [nucl-ex]].
[12] S. Baunack *et al.*, "Measurement of Strange Quark Contributions to the Vector Form Factors of the Proton at $Q^2 = 0.22\,(\mathrm{GeV/c})^2$," Phys. Rev. Lett. **102**, 151803 (2009) [arXiv:0903.2733 [nucl-ex]].
[13] Z. Ahmed *et al.* [HAPPEX Collaboration], "New Precision Limit on the Strange Vector Form Factors of the Proton," Phys. Rev. Lett. **108**, 102001 (2012) [arXiv:1107.0913 [nucl-ex]].
[14] W. J. Marciano and J. L. Rosner, "Atomic parity violation as a probe of new physics," Phys. Rev. Lett. **65**, 2963 (1990).
[15] M. J. Musolf, T. W. Donnelly, J. Dubach, S. J. Pollock, S. Kowalski and E. J. Beise, "Intermediate-energy semileptonic probes of the hadronic neutral current," Phys. Rept. **239** (1994) 1.
[16] D. B. Kaplan and A. Manohar, "Strange Matrix Elements in the Proton from Neutral Current Experiments," Nucl. Phys. B **310**, 527 (1988).
[17] R. D. Mckeown, "Sensitivity of Polarized Elastic electron Proton Scattering to the Anomalous Baryon Number Magnetic Moment," Phys. Lett. B **219**, 140 (1989).
[18] D. H. Beck, "Strange Quark Vector Currents and Parity Violating Electron Scattering From the Nucleon and From Nuclei," Phys. Rev. D **39**, 3248 (1989).
[19] J. Erler and M. J. Ramsey-Musolf, "The Weak mixing angle at low energies," Phys. Rev. D **72**, 073003 (2005) [arXiv:hep-ph/0409169].
[20] J. Liu, R. D. McKeown and M. J. Ramsey-Musolf, "Global Analysis of Nucleon Strange Form Factors at Low Q^2," Phys. Rev. C **76**, 025202 (2007) [arXiv:0706.0226 [nucl-ex]].
[21] T. A. Forest, "A Measurement of the Proton Weak Magnetic Form Factor (G_M^Z) at $Q^2 = 0.1\,\mathrm{GeV}^2$," For SAMPLE Collaboration.
[22] D. S. Armstrong, R. D. McKeown, "Parity-Violating Electron Scattering and the Electric and Magnetic Strange Form Factors of the Nucleon," Ann.Rev.Nucl.Part.Sci. **62** (2012) 337-359.
[23] R. González-Jiménez, J. A. Caballero and T. W. Donnelly, "Global analysis of parity-violating asymmetry data for elastic electron scattering," Phys. Rev. D **90**, no. 3, 033002 (2014) [arXiv:1403.5119 [nucl-th]].
[24] R. D. Young, J. Roche, R. D. Carlini and A. W. Thomas, "Extracting nucleon strange and anapole form factors from world data," Phys. Rev. Lett. **97**, 102002 (2006) [arXiv:nucl-ex/0604010].
[25] R. S. Sufian, Y. B. Yang, A. Alexandru, T. Draper, K. F. Liu and J. Liang, "Strange Quark Magnetic Moment of the Nucleon at Physical Point," arXiv:1606.07075 [hep-ph].
[26] R. S. Sufian, G. F. de Téramond, S. J. Brodsky, A. Deur and H. G. Dosch, "Analysis of Nucleon Electromagnetic Form Factors from Light-Front Holographic QCD : The Space-Like Region," arXiv:1609.06688 [hep-ph].
[27] S. J. Brodsky and G. F. de Téramond, "Hadronic spectra and light-front wavefunctions in holographic QCD," Phys. Rev. Lett. **96**, 201601 (2006) [arXiv:hep-ph/0602252].

[28] G. F. de Téramond and S. J. Brodsky, "Light-Front Holography: A First Approximation to QCD," Phys. Rev. Lett. **102**, 081601 (2009) [arXiv:0809.4899 [hep-ph]].

[29] G. F. de Téramond, H. G. Dosch and S. J. Brodsky, "Kinematical and Dynamical Aspects of Higher-Spin Bound-State Equations in Holographic QCD," Phys. Rev. D **87**, no. 7, 075005 (2013) [arXiv:1301.1651 [hep-ph]].

[30] G. F. de Téramond, H. G. Dosch and S. J. Brodsky, "Baryon spectrum from superconformal quantum mechanics and its light-front holographic embedding," Phys. Rev. D **91**, 045040 (2015) [arXiv:1411.5243 [hep-ph]].

[31] S. J. Brodsky, G. F. de Téramond, H. G. Dosch and C. Lorcé, "Universal effective hadron dynamics from superconformal algebra," Phys. Lett. B **759**, 171 (2016) [arXiv:1604.06746 [hep-ph]].

[32] A. Deur, S. J. Brodsky and G. F. de Teramond, "The QCD Running Coupling," Nucl. Phys. **90**, 1 (2016) [arXiv:1604.08082 [hep-ph]].

[33] S. J. Brodsky, G. F. de Teramond and A. Deur, "Nonperturbative QCD Coupling and its β-function from Light-Front Holography," Phys. Rev. D **81**, 096010 (2010) [arXiv:1002.3948 [hep-ph]].

[34] H. G. Dosch, G. F. de Téramond and S. J. Brodsky, "Superconformal Baryon-Meson Symmetry and Light-Front Holographic QCD," Phys. Rev. D **91**, no. 8, 085016 (2015) [arXiv:1501.00959 [hep-th]].

[35] G. F. de Téramond, "Hadron Physics From Superconformal Quantum Mechanics and its Light-Front Holographic Embedding," Few Body Syst. **57**, no. 10, 925 (2016) [arXiv:1601.05475 [hep-th]].

[36] S. J. Brodsky, G. F. De Téramond and H. G. Dosch, "Threefold Complementary Approach to Holographic QCD," Phys. Lett. B **729**, 3 (2014). [arXiv:1302.4105 [hep-th]].

[37] J. M. Maldacena, "The Large N limit of superconformal field theories and supergravity," Int. J. Theor. Phys. **38**, 1113 (1999) [Adv. Theor. Math. Phys. **2**, 231 (1998)] [arXiv:hep-th/9711200].

[38] S. J. Brodsky, G. F. de Téramond, H. G. Dosch and J. Erlich, "Light-Front Holographic QCD and Emerging Confinement," Phys. Rept. **584**, 1 (2015) [arXiv:1407.8131 [hep-ph]].

[39] J. J. Sakurai, "Theory of strong interactions," Annals Phys. **11**, 1 (1960).

[40] S. J. Brodsky and G. R. Farrar, "Scaling Laws at Large Transverse Momentum," Phys. Rev. Lett. **31**, 1153 (1973).

[41] V. A. Matveev, R. M. Muradian and A. N. Tavkhelidze, "Automodellism in the large - angle elastic scattering and structure of hadrons," Lett. Nuovo Cim. **7**, 719 (1973).

[42] G. F. de Téramond, "The spectroscopy and form factors of nucleon resonances from superconformal quantum mechanics and holographic QCD," Few Body Syst. **57**, 925 (2016) [arXiv:1602.04899 [hep-ph]].

[43] G. F. de Teramond and S. J. Brodsky, "Hadronic Form Factor Models and Spectroscopy Within the Gauge/Gravity Correspondence," arXiv:1203.4025 [hep-ph].

[44] Y. Aoki, *et al.* [RBC and UKQCD Collaborations],"Continuum Limit Physics from 2+1 Flavor Domain Wall QCD," Phys. Rev. D **D93**, (2011) 074508 [arXiv:1011.0892 [hep-lat]].

[45] T. Blum, *et al.* [RBC and UKQCD Collaborations], "Domain wall QCD with physical quark masses," Phys.Rev. **D93** (2016) 074505 [arXiv:1411.7017 [hep-lat]].

[46] R. J. Hill and G. Paz, "Model independent extraction of the proton charge radius from electron scattering," Phys.Rev. **D82** (2010) 113005, arXiv:1008.4619 [hep-ph].

[47] Z. Epstein, G. Paz, and J. Roy, "Model independent extraction of the proton magnetic radius from electron scattering," Phys.Rev. **D90** (2014) 074027, arXiv:1407.5683 [hep-ph].

[48] T. R. Hemmert, B. Kubis, and U.-G. Meissner, "Strange chiral nucleon form-factors," Phys.Rev. **C60** (1999) 045501, arXiv:nucl-th/9904076 [nucl-th].

[49] B. C. Tiburzi, "Finite Volume Effects on the Extraction of Form Factors at Zero Momentum," Phys. Rev. D **90**, no. 5, 054508 (2014) [arXiv:1407.4059 [hep-lat]].

[50] M. J. Musolf and H. Ito, "Chiral symmetry and the nucleon's vector strangeness form-factors," Phys. Rev. C **55**, 3066 (1997) [arXiv:nucl-th/9607021].

[51] T. R. Hemmert, U.-G. Meissner, and S. Steininger, "Strange magnetism in the nucleon," Phys.Lett. **B437** (1998) 184–190, arXiv:hep-ph/9806226 [hep-ph].

[52] J.-W. Chen and M. J. Savage, "Baryons in partially quenched chiral perturbation theory," Phys.Rev. **D65** (2002) 094001, arXiv:hep-lat/0111050 [hep-lat].

[53] Silas R. Beane, "Nucleon Masses and Magnetic Moments in a Finite Volume," Phys. Rev. **D70**, (2004) 034507 [arXiv:hep-lat/0403015].

[54] S. L. Zhu, S. J. Puglia, B. R. Holstein and M. J. Ramsey-Musolf, "The Nucleon anapole moment and parity violating e p scattering," Phys. Rev. D **62**, 033008 (2000) [arXiv:hep-ph/0002252].

[55] A. Silva, H. C. Kim and K. Goeke, "Strange form-factors in the context of SAMPLE, HAPPEX, and A4 experiments," Phys. Rev. D **65**, 014016 (2002) [arXiv:hep-ph/0107185].

[56] A. Silva, H. C. Kim and K. Goeke, "Strange vector form-factors in the context of the SAMPLE, A4, HAPPEX and G0 experiments," Nucl. Phys. A **721**, 417 (2003) [arXiv:hep-ph/0211439].

[57] M. J. Ramsey-Musolf, Eur. Phys. J. A **24S2**, 197 (2005) [arXiv:nucl-th/0501023].